

A multivariate robust parameter design approach for optimization of AISI 52100 hardened steel turning with wiper mixed ceramic tool

A.P. Paiva, P.H. Campos, J.R. Ferreira, L.G.D. Lopes, E.J. Paiva, P.P. Balestrassi*

Industrial Engineering Institute, Federal University of Itajuba, Minas Gerais, Brazil

ARTICLE INFO

Article history:

Received 1 March 2011

Accepted 3 August 2011

Keywords:

Hard turning

Wiper ceramic tool

Multivariate Robust Parameter Design (MRPD)

Principal Component Analysis (PCA)

ABSTRACT

This paper presents an experimental study of AISI 52100 hardened steel turned with wiper mixed ceramic ($\text{Al}_2\text{O}_3 + \text{TiC}$) inserts coated with TiN, using Multivariate Robust Parameter Design (MRPD). The main characteristic of this new optimization approach consists of considering both controllable (x_i) and noise (z_i) variables of the hard turning process to find out the parameter levels which minimize the distance of each response (y_i) from its respective targets (T_i) while keeps each variance caused by the noise variables as low as possible. Using a crossed array, a response surface design formed by cutting speed (Vc), feed rate (f) and depth of cut (d) is submitted to the influence of four scenarios built with an 2^2 full factorial design of two noise factors – workpiece hardness decreasing (Z_1) and tool flank wear (Z_2). This experimental arrangement allows the generating of mean, variance and mean square error (MSE) of five surface roughness parameters (Ra, Rz, Ry, Rt and Rq). As these responses are highly correlated, to extract and employ this information, Principal Component Analysis (PCA) was used. Adopting the Multivariate Mean Square Error (MMSE) as optimization criteria, a robust solution could be found. Theoretical and experimental results were convergent and confirmed. With Vc = 199.9 m/min, f = 0.191 mm/rev and d = 0.190 mm, the five surface roughness parameters and respective variances were minimal, with better results than those obtained with individual optimization.

© 2011 Elsevier Ltd. All rights reserved.

1. Introduction

Considerable attention has been given recently to the understanding of hardened steel machining [1–17]. The hard turning process shows several potential benefits over traditional grinding – mainly considering its efficiency in the reduction of processing time consumed in each operation – such as, production costs [6], setup time [3,4], coolant elimination and reduced energy consumption [2], improvement of material properties, and capacity to promote low values for surface finish while removing much more workpiece material in a single cut rather than a lengthy grinding operation [4]. These benefits, however, can only be achieved with adequate values for the process parameters as also the correct choice of tool material and geometry [4].

Related to the contribution of the tool geometry for the improvement of hard turning process, several works present the use of wiper inserts as a machining tool [2,4,5]. This kind of insert allows the utilization of a much higher feed rate on the turning process when compared with traditional tools, due to its three radii geometry [4], with two of them being disposed adjacent to the nose radius with little or no clearance angle. This characteristic improves the finishing by the greater burnishing of the machined surface. With this

modification in the tool nose geometry it is possible to double the feed rate, increasing the productivity and also keeping the surface roughness as low as possible. Gaitonde et al. [2], studying the effects of cutting parameters in a hard turning operation, confirmed that wiper mixed ceramic inserts presented better surface roughness and tool wear performance when compared with traditional turning operation of high chromium AISI D2 cold work tool steel. Also in the AISI D2 steels with 60 HRC, Ozel et al. [4] indicate that the average surface roughness (Ra) is attainable with wiper tools, with values around 0.20 μm .

The potential benefits promoted by hard turning for surface quality and the increasing of productivity rate depend intrinsically on an optimal setup for the process parameters such as cutting speed (Vc), feed rate (f) and depth of cut (d). These parameters are directly responsible for many of machining predictable properties like tool wear, tool life, surface finishing and amount of material removed [4]. In this sense, trying to achieve a better hard turning process comprehension, several works has been done recently [1–24]. Some works have studied the effect of cutting conditions (Vc, f, d) [1–4,6,7], the influence of workpiece hardness [1], the tool geometry on surface roughness and cutting forces [1,4,10,11], the effects of cutting fluids [12–14], the wear and tribochemical mechanisms [8], the tool flank wear and its influence to the geometric error as the influence of solid lubricants [17], the surface integrity (surface roughness, residual stress and thermal damage layer) [18], the cooling effects [19] and the

* Corresponding author. Tel.: +55 865 978 8385.

E-mail addresses: pedro@unifei.edu.br, balestrassi@tennessee.edu (P.P. Balestrassi).

accuracy and thermal damage [20,21]. Most of these works attempt to establish a relationship between process output properties (tool life, surface roughness, cutting forces) and inputs variables (cutting speed, feed rate and depth of cut).

To model the machining properties as function of hard turning process parameters, many researchers have used Response Surface Methodology (RSM) [1,3,6,7,14,21–28]. In this methodology, the effect of cutting parameters on machining outputs are obtained using a set of experiments capable of generate an appropriate dataset for efficient statistical analysis, which in turn produces valid and objective models [29]. These models can be used in optimization, simulation or prediction of turning process behavior, mainly within the experimental range [6,7,29]. Bouacha et al. [1] used RSM to build quadratic models for surface roughness and cutting forces in the study of AISI 52100 hardened bearing steel. After the modeling task, desirability function was used as a multiresponse optimization method. Mandal et al. [3] employed RSM to study flank wear of Zirconia Toughened Alumina and used desirability function to minimize tool wear as a function of cutting speed levels, feed rate and depth of cut. Benga and Abrão [26] have studied tool life and the surface finishing of hardened 100Cr6 bearing steel obtained with PCBN and ceramic inserts using RSM. Singh and Rao [10] conducted an experimental investigation for the effects of cutting conditions and tool geometry on the surface roughness of the bearing steel (AISI 52100) with mixed ceramic inserts made of aluminum oxide and titanium carbonitride (SNGA), having different nose radius and different effective rake angles. Sahin and Motorcu [22] used RSM to model surface roughness (Ra, Rz and Rmax) in the turning of AISI 1050 hardened steels by cubic boron nitride (CBN) cutting tools. Al-Ahmari [24] built empirical models for tool life, surface roughness and cutting force in a hard turning of austenitic AISI 302.

Most of the literature on machining process presents some kind of multiresponse modeling and optimization. In a great number of papers, researchers prefer a routine based on the composite desirability function [30] to find optimum values of machining parameters with respect to its targets when more than one characteristic is needed [1,3,14]. Iqbal et al. [14], for example, used the desirability approach to simultaneously maximize tool life (y_1) and to minimize average surface roughness measured along (y_2) and across (y_3) (where y_2 and y_3 were feed directions in the milling of AISI D2 and in the X210 Cr12 steels). To model the effects of cutting parameters applied to the finish of hard-milling process with MQL (Minimum Quantity of Lubricant), researchers have used a D-optimal response surface design. The desirability method, however, present large limitations in terms of correlation influences over the optimization [37].

Besides, all aforementioned works are related only with the use of RSM for the modeling of mean values of the machining properties, neglecting in this case effect that noise factors may cause in the performance of the machining process. This effect can be mathematically expressed as of a variance equation. Assuming that noise factors can be controlled in an experimental environment, the determination of the level of controllable factors that makes the processes less sensitive to the variation caused by the noise ones can be reached through an optimization approach called Robust Parameter Design (RPD) [31–34]. So, considering that mean value ($\hat{\mu}$) of machining outputs must reach its target (θ) while variance ($\hat{\sigma}^2$) is simultaneously reduced, a Dual Response Surface (DRS) is generally considered to attain the proposed goals in each quality characteristic. This task is accomplished by building a response surface for mean, variance or alternatively by its combination, called Mean Square Error (MSE). According to Lin and Tu [33] and Vining and Myers [35] the minimization of MSE can be considered an efficient optimization strategy for RPD. In mathematical terms, MSE combines response surface for $\hat{\mu}$ (mean) and $\hat{\sigma}^2$ (variance) related to θ (target) as:

$$MSE = (\hat{\mu} - \theta)^2 + \hat{\sigma}^2. \quad (1)$$

Alternatively, supposing that MSE can be calculated within experimental results for each experimental run in the response surface design, one can directly establish a model for MSE. Eq. (1) represents the mean square error of a unique output. By considering that the hardened steel machining processes have many characteristics to be improved than the dual optimization described by Eq. (1) it is not enough to promote solutions to the entire set of characteristics. Extending the MSE criterion to optimize multiple responses, Kksoy [34] and Kksoy and Yalcinoz [36] have proposed the agglutination of mean square error of each response using a weighted sum (or the most important MSE response) as objective function while the remaining were kept as constraints. Although efficient, this method ignores the correlation that multiple means and variances can exhibit. The presence of correlation can cause model's instability, overfitting of prediction equations and an inaccuracy on regression coefficients. This means that regression equations are not adequate to represent a global objective function without considering the variance-covariance structure among multiple responses [37–39]. Some optimization approaches concerned with correlation among multiple responses were recently established [6,7,37–46], but they were not capable of treat dual response surface (DRS) problems.

Therefore, as most part of machining processes presents large sets of correlated responses [46] that are generally influenced by noise variables, in this paper we will propose a multiobjective optimization method for correlated mean square error functions based on the concept of multivariate mean square error (MMSE) established by Paiva et al. [7]. Using a crossed array, a response surface design formed by cutting speed (V_c), feed rate (f) and depth of cut (d) is submitted to the influence of several scenarios built with an full factorial design of two noise factors – workpiece hardness (Z_1) and tool flank wear (Z_2). This experimental arrangement allows the generation of mean, variance and mean square error (MSE) for five surface roughness parameters (Ra, Rz, Ry, Rt and Rq). As these responses are highly correlated, this information can be extracted using Principal Component Analysis (PCA) and will integrate the MMSE function. This approach will be called herein Multivariate Robust Parameter Design (MRPD). The next section describes how this approach can be developed by the practitioners

2. Multivariate Robust Parameter Design

A multiobjective optimization problem, also considering inequality constraints, can be stated as Eq. (2):

$$\begin{aligned} & \text{Minimize } f_1(\mathbf{x}), f_2(\mathbf{x}), \dots, f_p(\mathbf{x}) \\ & \text{Subject to : } g_j(\mathbf{x}) \leq 0, \quad j = 1, 2, \dots, m. \end{aligned} \quad (2)$$

Suppose that $f_1(\mathbf{x}), f_2(\mathbf{x}), \dots, f_p(\mathbf{x})$ are correlated with values written in terms of a random vector $Y^T = [Y_1, Y_2, \dots, Y_p]$. Assuming that Σ is the variance-covariance matrix associated to this vector then Σ can be factorized in pairs of eigenvalues-eigenvectors $(\lambda_i, e_i), \dots \geq (\lambda_p, e_p)$, where $\lambda_1 \geq \lambda_2 \geq \dots \geq \lambda_p \geq 0$, such as the i th uncorrelated linear combination may be stated as $PC_i = e_i^T Y = e_{i1}Y_1 + e_{i2}Y_2 + \dots + e_{ip}Y_p$ with $i = 1, 2, \dots, p$ [47]. This uncorrelated linear combination is called principal component score and can be obtained using PCA [47]. This algorithm is available in many statistical packages in a larger deal of user friendly displays. In the Minitab® 15.0, for example, the principal component scores can be directly stored in a worksheet column.

Relating these concepts to the MRPD approach aforementioned discussed, let's suppose that the multiple calculated MSE_{ij} dataset can be replaced by this uncorrelated linear combination. Then, a multiobjective function can be written aggregating the several responses into a unique index while keeps its variance-covariance structure and the individual deviation from each target. At this point, we will use the MMSE concept [7].

Multivariate Mean Square Error (MMSE) is a multivariate dual response surface criterion developed by replacing the estimated mean \hat{y} by an estimated principal component score regression (PC_i) and the estimated variance $\hat{\sigma}^2$ by the respective eigenvalue λ_i [7]. Taking ζ_{PC_i} as the target for the i -th principal component, a multivariate mean square error formulation can be defined as:

$$MMSE_i = (PC_i - \zeta_{PC_i})^2 + \lambda_i. \tag{3}$$

In Eq. (3) PC_i is the fitted second-order polynomial for principal component score, ζ_{PC_i} is the target value of the i -th principal component that must keep a straightforward relation with the targets of the original data set. This relationship may be established using Eq. (4) such as:

$$\zeta_{PC_i} = e_i^T [Z(Y_p | \zeta_{Y_p})] = \sum_{i=1}^p \sum_{j=1}^q e_{ij} [Z(Y_p | \zeta_{Y_p})] \quad i = 1, 2, \dots, p; \tag{4}$$

$$j = 1, 2, \dots, q.$$

In Eq. (4) e_i are the eigenvectors associated to the i -th principal component and ζ_{Y_p} represents the target for each of the p original responses. With this transformation, it can be established a coherent value for the target of the i -th principal component, that is compatible with the targets of the original problem.

Suppose now that $Y_p = MSE_p = (\mu_p - \theta)^2 + \sigma_p^2$. Then, if more than one principal component will be necessary, using the MMSE functions whose eigenvalues are equal or greater than the unity, we may write a multiobjective problem in the following form:

$$\text{Minimize } MMSE_T = \left[\prod_{i=1}^k (MMSE_i | \lambda_i \geq 1) \right]^{\left(\frac{1}{k}\right)} \tag{5}$$

$$= \left\{ \prod_{i=1}^k \left[(PC_i - \zeta_{PC_i})^2 + \lambda_i | \lambda_i \geq 1 \right] \right\}^{\left(\frac{1}{k}\right)}$$

$$i = 1, 2, \dots, k; \quad k \leq p.$$

$$\text{Subject to : } \mathbf{x}^T \mathbf{x} \leq \rho^2 \tag{6}$$

$$\hat{g}_i(\mathbf{x}) \leq 0. \tag{7}$$

$$\text{With : } \zeta_{PC_i} = e_{1i} [Z(MSE_1 | \zeta_{MSE_1})] + e_{2i} [Z(MSE_2 | \zeta_{MSE_2})] \tag{8}$$

$$+ \dots + e_{pi} [Z(MSE_p | \zeta_{MSE_p})]$$

$$PC_i = b_{0i} + [\nabla f(\mathbf{x})^T]_i + \left\{ \frac{1}{2} \mathbf{x}^T [\nabla^2 f(\mathbf{x})] \mathbf{x} \right\}_i \quad i = 1, 2, \dots, p. \tag{9}$$

$$MSE_p = (\hat{y}_p - \theta_p)^2 + \hat{\sigma}_p^2 \quad i = 1, 2, \dots, p. \tag{10}$$

To the better understanding, the practitioner may use the following procedure to replicate the proposed methodology, explored step by step in the next session:

2.1. Procedure

Step 1. Experimental design

Calculate mean and variance for each surface roughness metric (\hat{y}_i) obtained with a crossed array;

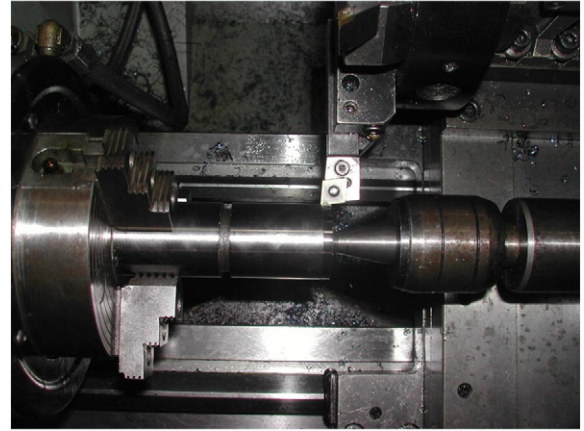


Fig. 1. Hard turning process with wiper ceramic tool.

Step 2. Modeling of responses

Establish equations for (\hat{y}_i) using experimental and calculated data and a full quadratic model;

Step 3. Constrained optimization of Y

Establish surface roughness targets (θ_i), using the constrained minimization of each surface equation individually;

Step 4. Modeling of MSEs

With the targets of step 3, calculate each MSE_i , such as $MSE_{ij} = (\hat{y}_{ij} - \theta_i)^2 + \hat{\sigma}_{ij}^2$ and build a full quadratic model for each MSE_i ;

Step 5. Constrained optimization of MSEs

Establish targets for MSE_i (θ_i^*), using the constrained minimization for each adjusted response surface equation individually;

Step 6. Principal Component Analysis

Conduct the Principal Component Analysis (PCA) using the correlation matrix of MSE_i , storing the PC-Scores (whose explained variance is at least 80%) and respective eigenvalues and eigenvectors;

Step 7. Modeling of PC-scores

Build full quadratic models for the PC-scores of each component that must be kept in the analysis.

Table 1
Inner array: control factors and respective levels.

Control Factors	Symbol	Levels				
		-1.682	-1	0	1	1.682
Coded Units						
Cutting speed (m/min)	Vc	186.4	200	220	240	253.6
Feed rate (mm/rev)	f	0.132	0.20	0.30	0.40	0.468
Depth of cut (mm)	d	0.099	0.150	0.225	0.300	0.351

Table 2
Outer array: noise factors and respective levels.

Noise factor	Symbol	-1	+1
Workpiece hardness (HRC)	Z ₁	40	50
Tool flank wear VBmax (mm)	Z ₂	0	0.30

Table 3
Response surface crossed array for Ra.

Inner array: control factors			Replicates				Outer array: noise factors		
Vc	f	d	Ra ₁	Ra ₂	Ra ₃	Ra ₄	Z ₁	Z ₂	Properties
							Mean	Variance	MSE
–1.000	–1.000	–1.000	0.225	0.153	0.288	0.243	0.227	0.003194	0.003493
1.000	–1.000	–1.000	0.233	0.219	0.383	0.292	0.281	0.00553	0.010637
–1.000	1.000	–1.000	0.485	0.388	0.432	0.320	0.406	0.004879	0.043312
1.000	1.000	–1.000	0.463	0.382	0.465	0.236	0.386	0.011554	0.042618
–1.000	–1.000	1.000	0.252	0.177	0.339	0.252	0.255	0.004414	0.00642
1.000	–1.000	1.000	0.252	0.173	0.260	0.260	0.236	0.001775	0.002464
–1.000	1.000	1.000	0.526	0.357	0.408	0.327	0.404	0.007692	0.045393
1.000	1.000	1.000	0.445	0.412	0.383	0.303	0.386	0.003662	0.034506
–1.682	0.000	0.000	0.338	0.373	0.289	0.290	0.322	0.001631	0.01424
1.682	0.000	0.000	0.369	0.358	0.256	0.266	0.312	0.003567	0.01403
0.000	–1.682	0.000	0.167	0.095	0.365	0.219	0.211	0.013068	0.01307
0.000	1.682	0.000	0.508	0.534	0.445	0.396	0.471	0.003903	0.071937
0.000	0.000	–1.682	0.378	0.349	0.283	0.311	0.330	0.001749	0.016249
0.000	0.000	1.682	0.413	0.416	0.259	0.318	0.351	0.005847	0.025799
0.000	0.000	0.000	0.348	0.298	0.355	0.285	0.321	0.001222	0.013645
0.000	0.000	0.000	0.378	0.294	0.296	0.273	0.310	0.002138	0.012138
0.000	0.000	0.000	0.321	0.308	0.293	0.267	0.297	0.000543	0.008163
0.000	0.000	0.000	0.339	0.290	0.273	0.263	0.291	0.001159	0.007726
0.000	0.000	0.000	0.343	0.322	0.306	0.229	0.300	0.002466	0.010566

Step 8. Constrained optimization of PC-scores

Establish the targets for the PC scores using $\zeta_{PC_i} = \sum_{i=1}^p \sum_{j=1}^q e_{ij}[Z(MSE_p | \zeta_{V_p})]$;

Step 9. Generalized Reduced Gradient

Using the so called Generalized Reduced Gradient (GRG) algorithm, minimize $\left\{ \prod_{i=1}^k [(PC_i - \zeta_{PC_i})^2 + \lambda_i | \lambda_i \geq 1] \right\}^{\left(\frac{1}{k}\right)}$, using as constraints the experimental region, non-negative variances and other constraint $g_i(x)$ that the practitioner judges to be necessary, as Material Removal Rate (MRR), for example.

3. A follow along experiment

To accomplish with the goals of this paper, dry turning tests of the AISI 52100 steel, (1.03% C; 0.23% Si; 0.35% Mn; 1.40% Cr; 0.04% Mo; 0.11% Ni; 0.001% S; 0.01%) were conducted on a CNC lathe with maximum rotational speed of 4000 rpm and power of 5.5 kW and using Wiper mixed ceramic (Al₂O₃ + TiC) inserts (ISO code CNGA 120408

S01525WH) coated with a very thin layer of titanium nitride (TiN) (Sandvik-Coromant GC 6050). The workpieces used in the turning process were made with dimensions of Ø 49 mm × 50 mm. All of them were previously quenched and tempered. After this heat treatment, their hardness was between 49 and 52 HRC, up to a depth of 3 mm below the surface. The tool holder used in the experiments presented a negative geometry with ISO code DCLNL 1616H12 and entering angle $\chi_r = 95^\circ$. Fig. 1 represents the turning process of AISI 52100 used in this experimental study.

Step 1. Experimental design

Adopting this experimental condition, the workpieces were machined using the range of parameters as defined in Table 1. A sequential set of experimental runs was established using a Central Composite Design (CCD) built according to the design shown in Table 1. To study the influence of two noise factors (Z₁: workpiece hardness and Z₂: tool flank wear) as showed in Table 2, each experiment with controllable factors in the CCD were executed in a different scenario. These scenarios, which characterize the outer array, were designed according to a 2² full factorial design as shown in Table 3. The first experimental condition of outer array was carried out with

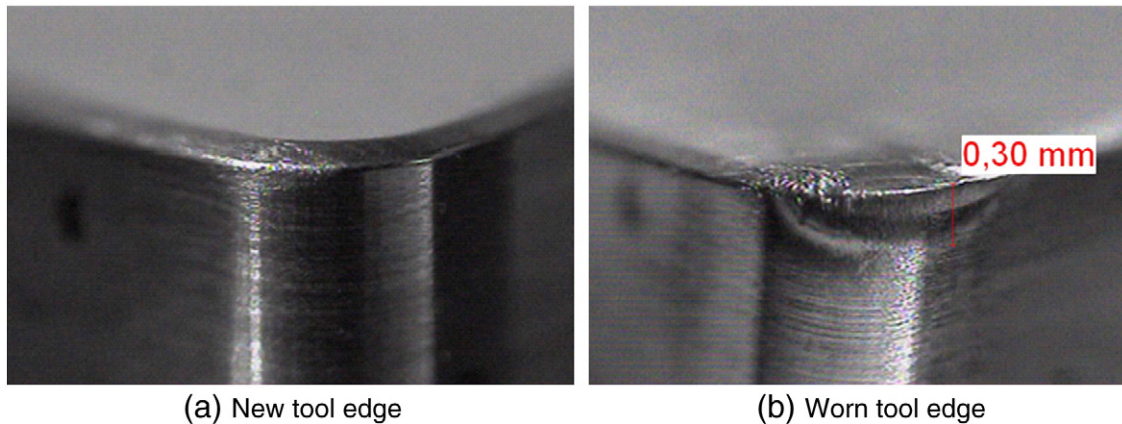


Fig. 2. Tool wear (noise factor levels).

Table 4
Surface roughness means and variances.

Run	Ra	Rz	Rt	Ry	Rq	Var ₁	Var ₂	Var ₃	Var ₄	Var ₅
1	0.227	1.254	1.455	1.406	0.278	0.00319	0.08517	0.14810	0.12287	0.00461
2	0.281	1.446	1.641	1.595	0.340	0.00553	0.13040	0.27502	0.23783	0.00784
3	0.406	2.306	3.131	3.077	0.553	0.00488	0.28340	1.01157	1.06995	0.01258
4	0.386	2.273	2.987	2.924	0.535	0.01155	0.71028	1.55357	1.52239	0.03301
5	0.255	1.336	1.557	1.530	0.312	0.00441	0.08466	0.21176	0.20534	0.00529
6	0.236	1.396	1.667	1.639	0.295	0.00177	0.09067	0.26055	0.27348	0.00278
7	0.404	2.044	2.657	2.539	0.523	0.00769	0.12102	0.28317	0.30485	0.01382
8	0.386	2.008	2.623	2.538	0.503	0.00366	0.07121	0.12672	0.12148	0.00652
9	0.322	1.744	2.034	1.989	0.412	0.00163	0.02488	0.02585	0.03769	0.00262
10	0.312	1.802	2.140	2.013	0.405	0.00357	0.04420	0.05074	0.04230	0.00511
11	0.211	1.378	1.685	1.597	0.270	0.01307	0.50613	0.74832	0.66784	0.02167
12	0.471	2.498	3.553	3.482	0.629	0.00390	0.09345	0.39983	0.43979	0.00479
13	0.330	1.835	2.148	2.118	0.417	0.00175	0.03747	0.02465	0.02915	0.00246
14	0.351	1.854	2.254	2.177	0.438	0.00585	0.09854	0.11829	0.11222	0.00776
15	0.321	2.142	2.644	2.591	0.434	0.00122	0.47660	1.42732	1.28338	0.00500
16	0.310	1.785	2.212	2.159	0.397	0.00214	0.04715	0.10425	0.10190	0.00346
17	0.297	1.727	1.919	1.906	0.433	0.00054	0.06307	0.09264	0.08931	0.01331
18	0.291	1.700	2.027	1.965	0.373	0.00116	0.04538	0.08940	0.07843	0.00254
19	0.300	1.759	2.163	2.102	0.389	0.00247	0.09263	0.23882	0.21077	0.00508

reduced diameters, obtained after several turning passes. In this condition, the material hardness decreases significantly, achieving a hardness of 40 HRC approximately [1]. The workpieces were, then, turned with a new tool edge (VB_{max} = 0.00 mm).

The second noise condition was carried out turning the full piece diameter with a new wiper tool edge (Fig. 2), with surface roughness parameters measured just after one pass. The remaining noise conditions were conducted using reduced and full piece diameters with worn tool edge (Fig. 2). Tool flank wear measurements (VB_{max}) were measured with an optical microscope (magnification 40×). These four noise conditions were established to simulate the general phenomena that occur when the practitioners carry out any turning operation, reproducing, in some sense, the decreasing of the hardness with the simultaneous tool edge wear. Obviously, in these conditions, the surface roughness value will suffer some kind of variation, independently of the control setup. So, the main objective of robust parameter design is to find out the control parameters setup capable of achieving a reduced surface roughness with minimal variance. The following surface roughness parameters were assessed using a Mitutoyo portable roughness meter model Surftest SJ 201 fixed to a cut-off length of 0.25 mm, arithmetic average surface roughness (R_a), maximum surface roughness (R_y), root mean square roughness (R_q), ten point height (R_z) and maximum peak to valley (R_t).

Using a Central Composite Design (CCD) as a response surface design, nineteen runs with four center points and axial distance of $\rho = 1.633$ were carried out measuring the surface roughness three times at four positions in the workpiece middle. With these results, mean and variance were calculated according to step 1 of our proposal (Tables 3 and 4).

The mean and variances values of these measurements are represented in Table 4.

According to the time series of Fig. 3, the simultaneous influence of the tool flank wear and the workpiece hardness decreasing is very large. It can be observed that the roughness (R_a and R_q) are extremely sensitive to changes in the noise conditions, causing instability in the process performance. This oscillation, expressed in terms of a non constant variance time series, causes productivity and capability losses due to the large total variance perceived. So, the surface roughness obtained with a new tool edge working over a hard material is an unrealistic scenario for decision making process, and represents a process performance valid only for the first passes.

Otherwise, the lower surface roughness obtained with worn tool edge it is not also a good reference, because in this condition the tool life is near to its end. Since the noise effect comes from uncontrollable factors, the robust parameter strategy is based on the levels findings of the controllable parameters (cutting speed, feed rate and

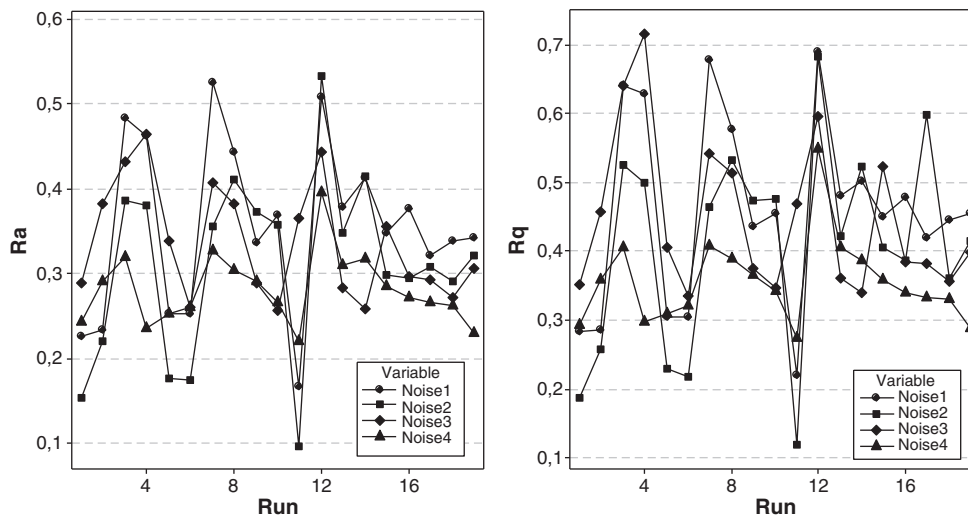


Fig. 3. Noise influence over experimental runs for Ra and Rq.

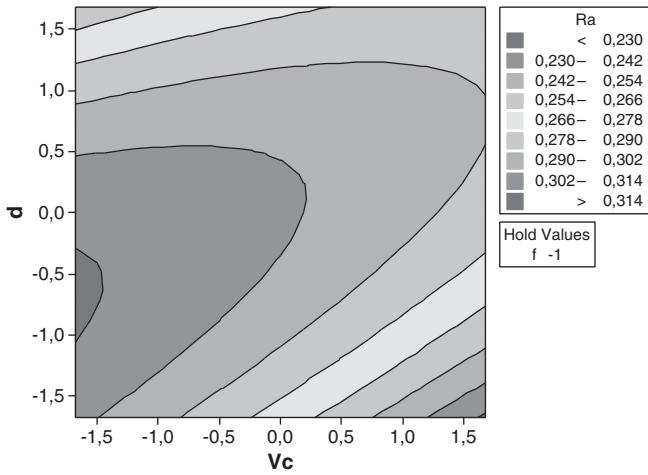


Fig. 4. Contour plots for Ra (coded units).

depth of cut, for example) which turn the performance less sensible to the variations caused by tool wear and workpiece hardness decreasing. Therefore, the main objective of MRPD approach is to minimize the distance of the responses performance from their targets while keeping the variances as lower as possible. This is the concept of robustness.

Step 2. Modeling of responses

With the experimental data, full quadratic models were considered for each surface roughness parameter, as suggested in step 2. Figs. 4 and 5 represent these models for Ra and Rq response surfaces. Table 5 presents the coefficients and the R-Sq (adj.) for each equation.

As can be observed in Table 5, feed rate is the most important factor to explain the average behavior of surface roughness. Although the remaining terms are not significant, they were kept in the model because their exclusion did not imply in prediction variance reduction (S term).

Step 3. Constrained optimization of Y

Considering then the full quadratic models \hat{y}_i , a nonlinear optimization system described by the Eqs. (11) and (12) can be implemented using the GRG Solver® routine available in the Excel package. After setting up the problem, the Solver® optimization parameters were chosen considering a precision of 10^{-6} , 100 iterations, a

Table 5
Regression coefficients and fits.

Coef.	Ra	Rz	Rt	Ry	Rq
Constant	0.3044	1.8265	2.1963	2.1476	0.4055
Vc	-0.0014	0.0204	0.0218	0.0136	-0.0005
f	0.0746	0.3722	0.6018	0.5914	0.1092
d	0.0011	-0.0338	-0.0390	-0.0480	-0.0028
Vc ²	0.0021	-0.0380	-0.0575	-0.0675	-0.0015
f ²	0.0106	0.0203	0.1305	0.1229	0.0131
d ²	0.0105	-0.0128	-0.0171	-0.0157	0.0051
Vc × f	-0.0092	-0.0401	-0.0593	-0.0566	-0.0102
Vc × d	-0.0089	-0.0170	0.0042	0.0091	-0.0101
f × d	0.0019	-0.0698	-0.1208	-0.1364	-0.0064
S	0.0151	0.1464	0.2133	0.2022	0.0238
R-Sq(adj)	94.98%	82.39%	86.01%	87.02%	94.10%

1 – Bold values represent the significant terms in the models (P-Value <5%).

quadratic estimative, forwards derivatives and the Newton's method as a line search option.

$$\text{Minimize } \hat{y}_i \tag{11}$$

$$\text{Subject to : } \mathbf{x}^T \mathbf{x} \leq \rho^2 \tag{12}$$

$$\hat{\sigma}_i^2 \geq 0.001.$$

Step 4. Modeling of MSEs

The constrained minimum will be the target (θ_i) to calculate each MSE_i , such as $MSE_{ij} = (\hat{y}_{ij} - \theta_i)^2 + \hat{\sigma}_{ij}^2$. These values are shown in Table 6.

According to the procedure established in the step 4, we employed the Ordinary Least Squares (OLS) algorithm to obtain the coefficients of a full quadratic model for MSE_i . These results are presented in Table 7 and Fig. 6.

Step 5. Constrained optimization of MSEs

The targets for each value of MSE_i (θ_i^*) can be obtained with a constrained minimization described by Eqs. (13) and (14). The results are shown in the Table 8. In these equations, each MSE_i is minimized under the spherical constraint (Eq. 13) and under the nonnegative constraint for mean square error. These targets are necessary in the multivariate approach.

$$\text{Minimize } MSE_i \tag{13}$$

$$\text{Subject to : } \mathbf{x}^T \mathbf{x} \leq \rho^2 \tag{14}$$

$$MSE_j \geq 0.001 \quad i \neq j.$$

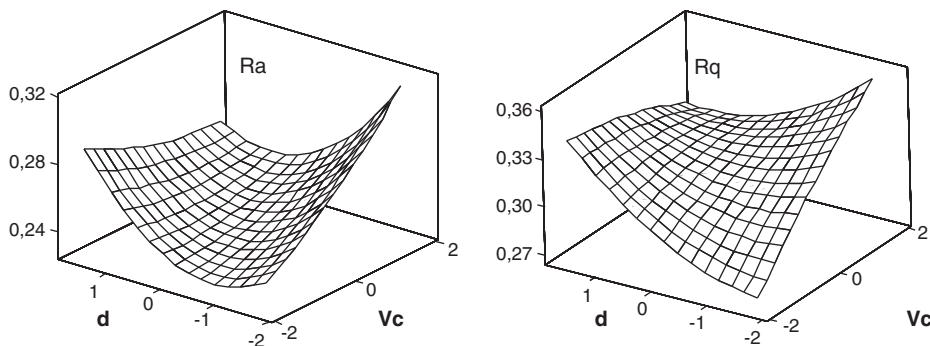


Fig. 5. Response surface plots for Ra and Rq.

Table 6
Mean square error for each response and first principal component score.

Run	MSE ₁	MSE ₂	MSE ₃	MSE ₄	MSE ₅	PC ₁	PC ₂
1	0.0035	0.0871	0.1493	0.1242	0.0054	-2.0267	0.1235
2	0.0106	0.1860	0.3241	0.2884	0.0159	-1.5600	-0.0974
3	0.0433	1.4838	3.9392	3.9827	0.1043	3.4790	0.3475
4	0.0426	1.8396	4.0093	3.9359	0.1140	3.8627	0.5421
5	0.0064	0.1006	0.2306	0.2308	0.0092	-1.8479	0.0290
6	0.0025	0.1251	0.3217	0.3460	0.0048	-1.9056	0.2813
7	0.0454	0.8172	1.8130	1.6713	0.0882	1.4446	-1.0186
8	0.0345	0.7072	1.5737	1.4855	0.0705	0.7750	-0.6133
9	0.0142	0.3100	0.4025	0.4209	0.0289	-1.1672	-0.2256
10	0.0140	0.3945	0.5691	0.4562	0.0291	-1.0400	-0.1132
11	0.0131	0.5342	0.8183	0.7195	0.0221	-0.8690	0.2092
12	0.0719	1.7527	4.9483	4.9007	0.1482	5.4441	-0.5302
13	0.0162	0.4276	0.5551	0.5891	0.0302	-0.9117	-0.1555
14	0.0258	0.5135	0.8138	0.7639	0.0429	-0.3456	-0.4761
15	0.0136	1.3454	2.9249	2.7738	0.0388	1.2651	1.5200
16	0.0121	0.3778	0.7313	0.7244	0.0251	-1.0087	0.0777
17	0.0082	0.3302	0.3414	0.3771	0.0467	-1.1295	-0.1974
18	0.0077	0.2859	0.4574	0.4320	0.0177	-1.4427	0.1241
19	0.0106	0.3944	0.7901	0.7464	0.0243	-1.0161	0.1730
Mean	0.0209	0.6323	1.3533	1.3141	0.0456	0.0000	0.0000
S. D.	0.0184	0.5568	1.4812	1.4676	0.0406	2.1614	0.5256
Z	-1.0277	-0.9631	-0.9130	-0.8948	-1.0474	-	-
Targets	0.0020	0.0959	0.0010	0.0010	0.0031	-2.1652	0.1502

Table 7
Regression coefficients and fits.

Coef.	MSE ₁	MSE ₂	MSE ₃	MSE ₄	MSE ₅	PC _{1(MSE)}	PC _{2(MSE)}
Constant	0.0106	0.5465	1.0422	1.0037	0.0305	-0.6679	0.3318
Vc	-0.0006	0.0375	0.0276	0.0078	-0.0001	0.0247	0.0601
f	0.0177	0.4685	1.2635	1.2534	0.0406	2.0150	-0.1700
d	0.0004	-0.1246	-0.2964	-0.3151	-0.0033	-0.3176	-0.2033
Vc ²	0.0006	-0.0674	-0.1617	-0.1636	-0.0005	-0.1459	-0.1377
f ²	0.0106	0.2123	0.6860	0.6749	0.0193	1.0531	-0.1345
d ²	0.0031	-0.0256	-0.0915	-0.0794	0.0022	0.0221	-0.1894
Vc×f	-0.0018	0.0153	-0.0544	-0.0640	-0.0018	-0.0869	0.0710
Vc×d	-0.0027	-0.0675	-0.0491	-0.0235	-0.0053	-0.1972	0.0855
f×d	-0.0001	-0.2189	-0.5801	-0.6158	-0.0065	-0.6194	-0.3507
S	0.0037	0.3577	0.8168	0.7749	0.0113	0.9002	0.4832
R-Sq(adj)	95.98%	58.72%	70.00%	72.11%	92.15%	82.65%	15.50%

Step 6. Principal Component Analysis

Although the responses are extremely and positively correlated, the solution that minimizes a specific MSE is not capable of minimizing the others. It can be observed in Table 9 that the solutions are quite different. In this work, bias is calculated as $\sum_{i=1}^p |MSE_i - MSE_T|$.

To consider the correlation among several MSE_i and to promote an agglutination objective function of these mean square error equations, the PCA algorithm must be driven. In this work, it was used the multivariate package available in the Minitab® 15.0. The results of this multivariate factorization (Eigenanalysis) are shown in the Table 9.

From Table 9, we can observe that the first two principal components represent 99.0% of the variance of the all MSE_i with respective

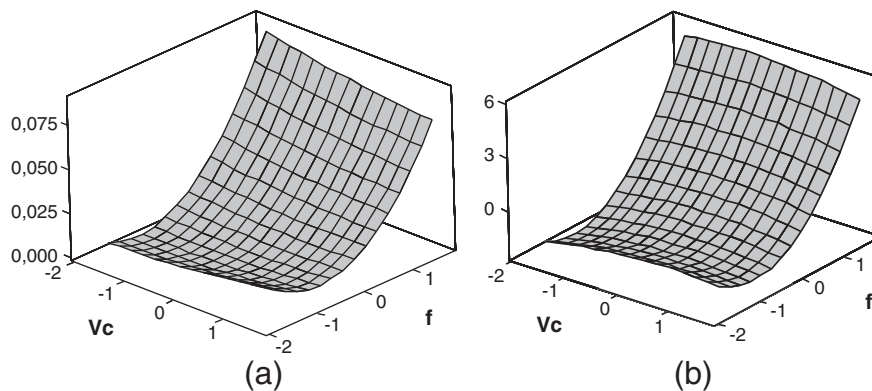


Fig. 6. Surface plots for (a) MSE₁ and (b) PC₁.

Table 8
Individual optimization results.

MSE ₁	MSE ₂	MSE ₃	MSE ₄	MSE ₅	Vc	f	d	Bias
0.001957	0.110286	0.019328	0.001000	0.003922	-1.132	-0.896	-0.461	0.1286
0.004809	0.095941	0.044117	0.001000	0.003872	-0.748	-1.360	-0.649	0.3300
0.005283	0.121449	0.001001	0.001001	0.007108	-0.640	-0.755	-1.273	0.1308
0.004980	0.116888	0.044109	0.001000	0.004791	-0.409	-1.215	-0.815	0.1668
0.002730	0.106169	0.032001	0.001000	0.003088	-0.939	-1.151	-0.511	0.1344

eigenvalues of $\lambda_1 = 4.672$ and $\lambda_2 = 0.276$. In practical terms, the principal component scores stored in the last two columns of **Table 8** (PC_1 (MSE); PC_2 (MSE)) were calculate as:

$$PC_k = \mathbf{Z}^T \mathbf{E} = \begin{bmatrix} \left(\frac{y_{11} - \bar{y}_1}{\sqrt{s_{11}}} \right) & \left(\frac{y_{21} - \bar{y}_2}{\sqrt{s_{22}}} \right) & \dots & \left(\frac{y_{p1} - \bar{y}_p}{\sqrt{s_{pp}}} \right) \\ \left(\frac{y_{12} - \bar{y}_1}{\sqrt{s_{11}}} \right) & \left(\frac{y_{22} - \bar{y}_2}{\sqrt{s_{22}}} \right) & \dots & \left(\frac{y_{p2} - \bar{y}_p}{\sqrt{s_{pp}}} \right) \\ \vdots & \vdots & \ddots & \vdots \\ \left(\frac{y_{1n} - \bar{y}_1}{\sqrt{s_{11}}} \right) & \left(\frac{y_{2n} - \bar{y}_2}{\sqrt{s_{22}}} \right) & \dots & \left(\frac{y_{pn} - \bar{y}_p}{\sqrt{s_{pp}}} \right) \end{bmatrix}^T \times \begin{bmatrix} e_{11} & e_{12} & \dots & e_{1p} \\ e_{21} & e_{22} & \dots & e_{2p} \\ \vdots & \vdots & \ddots & \vdots \\ e_{1p} & e_{2p} & \dots & e_{pp} \end{bmatrix} \quad (15)$$

Step 7. Modeling of PC-scores

The core of multivariate optimization is the transformation of original correlated responses (MSE_i in this case) in uncorrelated principal component scores. According to the theory, these components are capable of replace the original data in a few latent variables. In the present approach, these values can be used to generate a full quadratic model that replaces all MSE's. The principal component scores calculated as Eq. 15 are present in the **Table 6**. Applying the OLS algorithm we obtain the coefficient of principal component scores as describe in the **Table 7**.

Step 8. Constrained optimization of PC-scores

Using the relationship $\zeta_{PC_i} = \sum_{i=1}^p \sum_{j=1}^q e_{ij} [Z(Y_p | \zeta_{Y_p})]$ and the minimal values of individual optimization of MSE_i shown in **Table 9**, the principal component targets were calculated as $\zeta_{PC_1} = -2.1652$ and $\zeta_{PC_2} = 0.1502$. The minimization of the distance between each principal component and its respective target can lead to a compromise solution that attends the targets of all five correlated responses. Adopting these aspects and the minimization criteria, a nonlinear

Table 9
Eigenanalysis of the five MSE's.

Eigenvalue	4.67190	0.27630	0.03230	0.01910	0.00040
Proportion	0.93400	0.05500	0.00600	0.00400	0.00000
Cumulative	0.93400	0.99000	0.99600	1.00000	1.00000
<i>Eigenvectors</i>					
MSE1	0.431	-0.668	0.410	0.443	0.057
MSE2	0.448	0.414	-0.481	0.623	0.093
MSE3	0.455	0.321	0.334	-0.172	-0.741
MSE4	0.455	0.319	0.348	-0.369	0.659
MSE5	0.447	-0.421	-0.606	-0.500	-0.065

optimization system may be written in terms of the multivariate mean square error using, additionally, a spherical constraint to the factor levels. This constraint ($\rho^2 = 2.667$) will force the solution to fall within the experimental region. Gathering the previous information in a comprehensive optimization system, it is possible to write the following expressions:

$$\text{Minimize } MMSE_T = \sqrt{\left[(PC_1 - \zeta_{PC_1})^2 + \lambda_1 \right] \times \left[(PC_2 - \zeta_{PC_2})^2 + \lambda_2 \right]} \quad (16)$$

$$\text{Subject to : } \mathbf{x}^T \mathbf{x} \leq \rho^2 = Vc^2 + f^2 + d^2 \leq 2.667 \quad (17)$$

$$\text{With } \zeta_{PC_i} = e_{1i} [Z(MSE_1 | \zeta_{MSE_1})] + e_{2i} [Z(MSE_2 | \zeta_{MSE_2})] + e_{3i} [Z(MSE_3 | \zeta_{MSE_3})] + e_{4i} [Z(MSE_4 | \zeta_{MSE_4})] + e_{5i} [Z(MSE_5 | \zeta_{MSE_5})] \quad (18)$$

$$PC_i = b_{0i} + [\nabla f(\mathbf{x})^T]_i + \left\{ \frac{1}{2} \mathbf{x}^T [\nabla^2 f(\mathbf{x})] \mathbf{x} \right\}_i \quad (19)$$

$i = 1, 2, \dots, p.$

where: $\mathbf{x} = [Vc, f, d]$. The numerical values of the standardized targets $Z(MSE_i | \zeta_{MSE_i})$ were cited in the penultimate line of **Table 6**. The numerical values of eigenvectors e_{ij} for Eq. (18) are described in eigenanalysis of **Table 9**.

Step 9. Generalized Reduced Gradient

Using the GRG Solver® routine available in the Excel package again, we obtain the results available in the **Table 10**. Method “I” represents the solution obtained with only one principal component score regression, while in the Method “II” we use two components.

Fig. 7 shows the optimal solution found with MRPD in coded units. It is possible to verify that this solution (-1.005; -1.087; -0.469) attends all the constraint values imposed to the individual value of MSE. In uncoded units, this solution is Vc = 199.9 m/min, f = 0.191 mm/rev and d = 0.190 mm. It can be noticed that employing the MRPD approach, the bias is extremely reduced, indicating that the algorithm achieved an optimum which represents a compromise solution for means and variances, keeping the responses as close as possible from their targets. It can also be noticed that this is also different from that obtained in the individual constrained optimization.

The physical sense of the aforementioned results should be discussed to verify its consistence and for the better understanding and application of the methodology by researchers in machining or other manufacturing systems. Surface roughness is the greatness that quantifies the degree of workpiece finish. It is directly related

Table 10
MMSE optimization results.

Method	MSE ₁	MSE ₂	MSE ₃	MSE ₄	MSE ₅	Vc	f	d
I	0.00201	0.11017	0.02082	0.00100	0.00359	-1.052	-0.934	-0.518
II	0.00236	0.10843	0.02883	0.00100	0.00316	-1.005	-1.087	-0.469
Method	Ra	Rz	Rt	Ry	Rq	Vc	f	d
I	0.237	1.365	1.563	1.518	0.298	199.0	0.207	0.186
II	0.228	1.312	1.507	1.460	0.285	199.9	0.191	0.190
Method	Var (Ra)	Var (Rz)	Var (Rt)	Var (Ry)	Var (Rq)	Method	Bias	
I	0.003	0.1147	0.1609	0.1240	0.0050	I	0.03461	
II	0.004	0.1435	0.1890	0.1456	0.0062	II	0.04080	

to the tool geometry and machining parameters. Increasing radius of the tool tip, for example, tends to reduce roughness. This occurs into a certain limit, because increase in radius can cause vibrations, which contributes to worsen the finish. The feed rate is also a variable that directly influences the theoretical value of roughness, since the smaller is its value, the less likely will be the marks left on the workpiece surface by the passage of the tool. In practice, however, the surface finish is still influenced by the rake angle, the tool wear and the rigidity of the fixation system workpiece-tool. Apart from issues related to the cutting geometry, surface finish is little influenced by cutting speed.

Comparatively in hard turning, the influence of depth of cut is greater than the observed with the increase of cutting speed. When depth of cut is increased a greater capacity of material removal through the use of a greater portion of the cutting edge will be observed, but provoke increase of the thrust force and of the workpiece vibration and consequently worsen of the surface roughness. Therefore, considering the physical consequences of the optimized setup obtained with MRPD approach, we believe that $V_c = 199.9$ m/min, $f = 0.191$ mm/rev and $d = 0.190$ mm is an adequate setup for the surface finish operation of AISI 52100 hardened steel turned workpieces.

4. A comparative study

To compare the performance of wiper mixed ceramic tool obtained in this study and that obtained with conventional geometry tool, we will use the data present in [7]. In Paiva et al. [7], also using the MMSE method and a mixed ceramic tool (Al₂O₃ + TiC), ISO

code CNGA 120408 S01525 (Sandvik-Coromant CC6050) with conventional geometry, an average surface roughness $R_a = 0.40$ was reached, with a respective material removal rate of 6.43 cm³/s in the turning process of AISI 52100 hardened steel (53–55 HRC). These values were obtained with a cutting speed of 217.7 m/min, feed rate of 0.086 mm/rev and depth of cut of 0.342 mm. Table 11 shows that with wiper ceramic inserts in the machining of the same material, it can be used a feed rate more than twice larger than that achieved with conventional tool geometry and reached a lower surface roughness ($R_a = 0.228$). Besides, the productivity obtained with wiper ceramic tools are higher than the values obtained with conventional ones ($MRR = 7.43$ cm³/s).

Differently from the results with conventional geometry, the level of depth of cut was lower with wiper inserts. Since there is a relationship between machining force and the increase in the contact area between tool and workpiece furnished by the high values of depth of cut and feed rate. In the wiper case, it can be expected a lower wear rate, since the cutting forces have smaller growth than those obtained with

Table 11
Sensitivity analysis and comparison.

Tool geometry	Method	MRR	Ra	Vc	f	d
Conventional	Paiva et al. (2009)	6.43	0.400	217.7	0.080	0.340
Wiper	Proposed method (II)	7.34	0.228	199.9	0.191	0.190
	$g_1(x)$	8.0	0.243	197.0	0.216	0.186
	$g_2(x)$	9.0	0.245	193.9	0.219	0.211
	$g_3(x)$	10.0	0.253	194.0	0.227	0.227
	$g_4(x)$	12.0	0.270	201.5	0.240	0.270
Wiper	$g_5(x)$	15.0	0.276	211.3	0.242	0.295

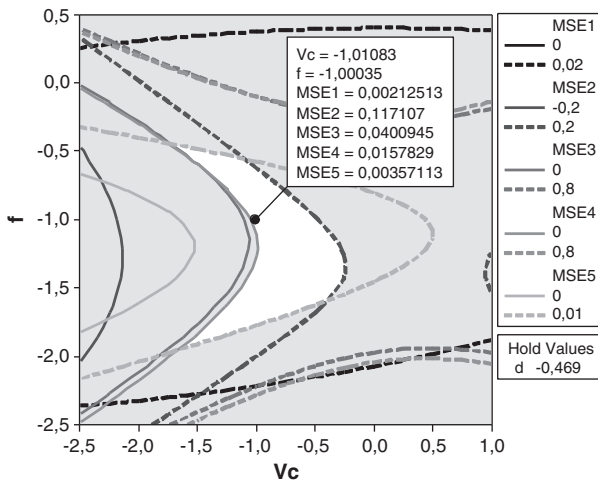


Fig. 7. Overlaid contour plot for each MSE.

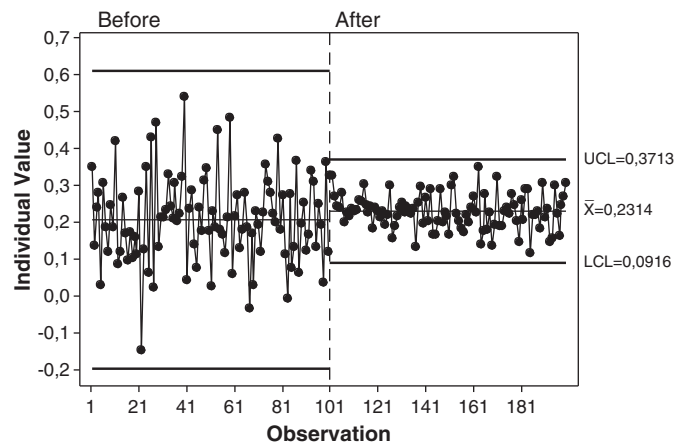


Fig. 8. Simulation runs for the current and optimal solutions (R_a).

Table 12
Predicted versus real values of surface roughness at optimum.

	Ra	Rz	Rt	Ry	Rq
Predicted mean	0.228	1.312	1.507	1.460	0.285
Real mean	0.227	1.340	1.215	1.377	0.276
Predicted S.D.	0.063	0.379	0.435	0.382	0.079
Real S. D.	0.050	0.359	0.288	0.369	0.061
Q1	0.190	1.053	0.980	1.080	0.230
Median	0.220	1.310	1.180	1.315	0.260
Q3	0.260	1.580	1.420	1.705	0.320

conventional inserts. As a sensitivity study, we added a new constraint to the optimization problem related to the material removal rate. As the surface roughness is very small, we forced the solution to higher values of MRR, observing the variation of Ra, for example. Even doubling MRR, Ra still presents values considerably low if compared with the value obtained in Paiva et al. [7].

Besides the good results of Ra and MRR, the present work considers the influence of variances raised from noise factors over the performance of the characteristics of interest. So, using the obtained results it is possible to simulate and compare the quality of the robust solution. Fig. 8 presents a simulation of Ra before and after the optimization routine just to emphasize the effectiveness of the obtained results.

The scenario called “Before” was simulated using normal probability distribution for Ra with parameters (0.211; 0.114), respectively representing mean and variance of the smallest value of Ra (corresponding to experiment no. 11). It can be noticed that the correspondent MRR is 6.52 cm³/s, obtained with Vc = 220 m/min, f = 0.132 mm/rev and d = 0.225 mm.

The scenario called “After” represents a normal probability distribution for Ra under the optimized conditions. It can be verified that the variance is extremely reduced while Ra achieves values very close to the smallest value of experimental runs. Besides, the respective MRR is 12.6% larger (7.34 cm³/s) than the value obtained in the experiment with the lowest Ra. Experiment no. 11 also presents the large experimental variance for Rz, Rt and Ry, although the minimal values for surface roughness were related to the condition of Vc = 200 m/min, f = 0.20 mm/rev and d = 0.15 mm (Experiment no. 1).

This comparison using simulated data shows that the MRPD approach was effectiveness in the treatment of mean and variance of multiple correlated responses in this case. A strategy considering the use of an outer array, formed by a factorial design of the noise factors was really capable of generate a real source of variation for the study. We believe that the robust results are closer to the real situations than those approaches concerned only with the explanation and optimization of the mean characteristic.

Table 13
Anova one-way: Ra versus noise condition.

Source	DF	SS	MS	F	P-Value
Noise	3	0.315893	0.105298	120.66	0.000
Error	188	0.164069	0.000873		
Total	191	0.479962			
Level		N	Mean	StDev	
New Tool	(40 HRC)	48	0.29104	0.02890	
New Tool	(50 HRC)	48	0.22938	0.02794	
Used Tool	(40 HRC)	48	0.20396	0.02893	
Used Tool	(50 HRC)	48	0.18292	0.03222	

5. Confirmation runs

To analyze the effectiveness of the optimal setup found with the MRPD approach and to confirm the findings of the simulation study, a set of confirmation runs was carried out, turning four workpieces for each one of the four noise conditions. The five surface roughness metrics were measured twelve times at the middle of the bars, resulting in a dataset of 192 observations of each surface finish state. The main objective of these confirmation runs was to verify if the surface roughness variance is minimal with their mean values as close as possible to the established targets. Table 12 present the ANOVA One-Way of average surface roughness (Ra) obtained under the four noise conditions. Fig. 9 shows the 95% confidence intervals for each roughness mean obtained in the four noise conditions.

It is clear that, although the means of surface roughness metrics in each noise condition are different (P-value < 5%), their means are very low. This variation observed among the four sample means highlights that the noise influence was not totally removed from the process with the optimal setup. Nonetheless, the variances (and the standard deviation) are notably lower with the optimized solution than with those observed with the experiment with the lowest value for the surface roughness. We can also note in the Table 13 that the mean and the standard deviation for the 192 confirmation runs for each surface roughness metric were very close to the predicted ones.

Fig. 10 shows a comparison between the experimental (Exp) and optimal (Opt) data for each response. As can be observed in the boxplots of this figure, the variances obtained with the optimal setup are much smaller than those observed with the experimental run no. 11. Using a 5% significance level, a two sample-t test of hypothesis was conducted to verify the equality of the means between optimal and experimental trials.

As shown in the Table 14, for Ra, Rt and Ry, there is an equality between means (P-Value > 5%), which suggest that the optimization was capable to reach the values close to the minimal observed. For Rz and Rq (with P-values < 5%), however, the optimal setup conducted to

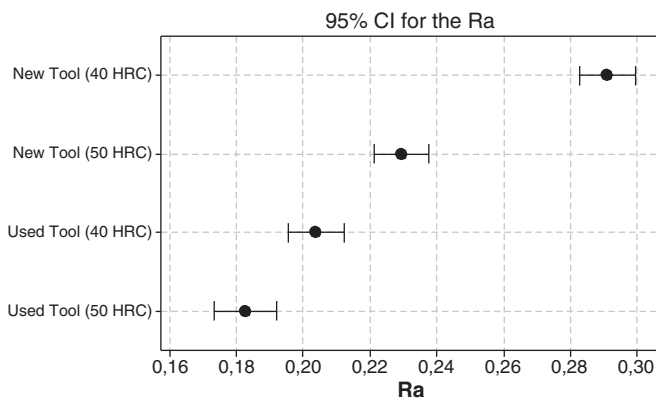


Fig. 9. ANOVA one-way: Ra versus noise condition.

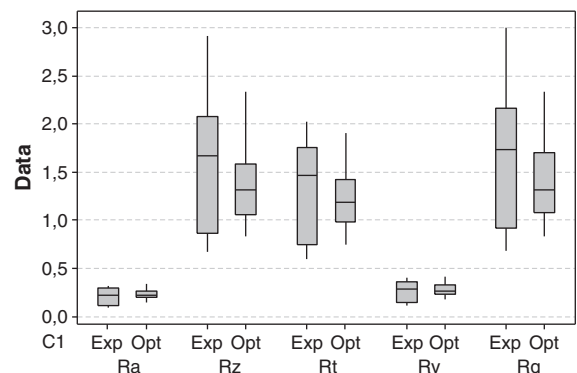


Fig. 10. Boxplot for comparison of variances of the surface roughness metrics.

Table 14
Hypothesis tests for means and variances.

Response		Mean	T	P-Value	S. D.	F	P-Value	Levene	P-Value
Ra	Opt	0.227	1.540	0.129	0.050	0.360	0.000	54.430	0.000
	Exp	0.208							
Rz	Opt	1.340	−2.530	0.014	0.359	0.330	0.000	28.150	0.000
	Exp	1.579							
Rt	Opt	1.215	−1.670	0.101	0.288	0.350	0.000	32.520	0.000
	Exp	1.337							
Ry	Opt	0.276	0.670	0.506	0.061	0.330	0.000	50.830	0.000
	Exp	0.265							
Rq	Opt	1.377	−2.730	0.009	0.369	0.330	0.000	30.420	0.000
	Exp	1.640							

smaller values for means than those seen at the experimental run. This test was used because the variances of each sample or level (experimental versus optimal) were not homogeneous. Accordingly, Table 14 also presents a test of hypothesis to verify the equality of variance in these cases. Considering a F-test (for normal distributions) or even a Levene test (for any continuous distribution), we observed that all p-values were smaller than the significance level, which indicates that the variances are statistically different, as was suggested by the boxplots of Fig. 10.

6. Conclusions

On the basis of the results presented, the following conclusions can be drawn:

1. The process optimization based on the Multivariate Robust Parameter Design approach (MRPD) in situations where the multiple responses exhibit a moderate to high degree of correlation, showed a consistent adequacy applied to the hard turning of AISI 52100 with wiper mixed ceramic tools.
2. The results and confirmatory runs allowed to state that MRPD approach outperforms the individual optimization routines, with minimal variance for each surface roughness parameter. The bias of each response is also extremely reduced with MRPD approach, indicating that the algorithm achieved an optimum which represents a compromise solution for means and variances, keeping the responses as close as possible from their targets.
3. In the turning process of AISI 52100 with wiper mixed ceramic tools, the first principal component was responsible for most of the variance-covariance present in the original data associated with the five surface roughness metrics. The second principal component was used as an alternative to improve the explanation of the surface roughness behavior of the machined parts.
4. Simultaneous optimization of the five responses of AISI 52100 hard steel turned with wiper mixed ceramic insert was achieved with a cutting speed of $V_c = 199.9$ m/min, feed rate of $f = 0.191$ mm/rev and depth of cut of $d = 0.190$ mm.
5. Comparing the presented results with those suggested in the literature with a conventional geometry for inserts, it was shown that with wiper inserts it can be used a feed rate more than twice larger than that achieved with conventional tool geometry, with a surface roughness that is nearly half ($R_a = 0.228$). Besides, the productivity obtained with wiper tools are higher than the value obtained with conventional ones ($MRR = 7.43$ cm³/s). Even relaxing the constraint associated with the MRR equation, the productivity is almost twice with low values for surface roughness.
6. For all responses, the values of surface roughness are low and the variance was extremely reduced.

Although the results are quite adequate, further works may include studies about the measurement, modeling and interpretation of the interaction effects that can occur between control and noise

variables. This can be done with a combined array. The present study can also be extended to other levels of workpiece hardness and for other insert substrate, as PCBN tools, with wiper and conventional geometry. Even considering the quality of results of the present approach, these conclusions cannot be extrapolated to different materials, tools or machine tools and they are valid only in the adopted range levels. It can, nonetheless, be recommended to be applied in many other manufacturing processes.

Acknowledgment

The authors would like to express their gratitude to FAPEMIG through project TEC APQ-01562-08, and also to CAPES and CNPq for their support in this research.

References

- [1] Bouacha K, Yaltese MA, Mabrouki T, Rigal JF. Statistical analysis of surface roughness and cutting forces using response surface methodology in hard turning of AISI 52100 bearing steel with CBN tool. *Int J Refract Met Hard Mater* 2010;28:349–61.
- [2] Gaitonde VN, Karnik SR, Figueira L, Davim JP. Machinability investigations in hard turning of AISI D2 cold work tool steel with conventional and wiper ceramic inserts. *Int J Refract Met Hard Mater* 2009;27:754–63.
- [3] Mandal N, Doloi B, Mondal B. Development of flank wear prediction model of Zirconia Toughened Alumina (ZTA) cutting tool using response surface methodology. *Int J Refract Met Hard Mater* 2011;29:273–80.
- [4] Ozel T, Karpat Y, Figueira L, Davim JP. Modelling of surface finish and tool flank wear in turning of AISI D2 steel with ceramic wiper inserts. *J Mater Process Technol* 2007;189:192–8.
- [5] Grzesik W. Wear development on wiper Al₂O₃-TiC mixed ceramic tools in hard machining of high strength steel. *Wear* 2009;266:1021–8.
- [6] Paiva AP, Ferreira JR, Balestrassi PP. A multivariate hybrid approach applied to AISI 52100 hardened steel turning optimization. *J Mater Process Technol* 2007;189:26–35.
- [7] Paiva AP, Paiva EJ, Ferreira JR, Balestrassi PP, Costa SC. A multivariate mean square error optimization of AISI 52100 hardened steel turning. *Int J Adv Manuf Technol* 2009;43:631–43.
- [8] Huang Y, Chou YK, Liang SY. CBN tool wear in hard turning: survey on research progresses. *Int J Adv Manuf Technol* 2007;35:443–53.
- [9] Tamizharasan T, Sevaraj T, Haq AN. Analysis of tool wear and surface finish in hard turning. *Int J Adv Manuf Technol* 2006;28:671–9.
- [10] Singh D, Rao PV. A surface roughness model for hard turning process. *Int J Adv Manuf Technol* 2007;32:1115–24.
- [11] Ozel T, Hsu TK, Zeren E. Effects of cutting edge geometry, workpiece hardness, feed rate and cutting speed on surface roughness and forces in finish turning of hardened AISI H13 steel. *Int J Adv Manuf Technol* 2005;25:262–9.
- [12] Lima JG, Ávila RF, Abrão AM, Faustino M, Davim JP. Hard turning: AISI 4340 high strength low alloy steel and AISI D2 cold work tool steel. *J Mater Process Technol* 2005;169:388–95.
- [13] Diniz AE, Ferreira JR, Filho FT. Influence of refrigeration/lubrication condition on SAE 52100 hardened steel turning at several cutting speeds. *Int J Mach Tools Manuf* 2003;42:317–26.
- [14] Iqbal A, Ning H, Khan I, Liang L, Dar NU. Modeling the effects of cutting parameters in MQL-employed finish hard-milling process using D-optimal method. *J Mater Process Technol* 2008;199:379–90.
- [15] Zhou JM, Andersson M, Stahl JE. The monitoring of flank wear on the CBN tool in the hard turning process. *Int J Adv Manuf Technol* 2003;22:697–702.
- [16] Quiza R, Figueira L, Davim JP. Comparing statistical models and artificial neural networks on predicting the tool wear in hard machining D2 AISI steel. *Int J Adv Manuf Technol* 2008;37:641–8.

- [17] Singh D, Rao PV. Performance improvement of hard turning with solid lubricants. *Int J Adv Manuf Technol* 2008;38:529–35.
- [18] Zhang XP, Liu CR, Yao Z. Experimental study and evaluation methodology on hard surface integrity. *Int J Adv Manuf Technol* 2007;34:141–8.
- [19] Haq AN, Tamizharasan T. Investigation of the effects of cooling in hard turning operations. *Int J Adv Manuf Technol* 2006;30:808–16.
- [20] Huang Y, Liang SY. Modelling of CBN Tool crater wear in finish hard turning. *Int J Adv Manuf Technol* 2004;24:632–9.
- [21] Özel T, Karpaz Y. Predictive modeling of surface roughness and tool wear in hard turning using regression and neural networks. *Int J Mach Tools Manuf* 2005;45:467–79.
- [22] Sahin Y, Motorcu AR. Surface roughness model in machining hardened steel with cubic boron nitride cutting tool. *Int J Refract Met Hard Mater* 2008;26:84–90.
- [23] Kwak JS, Sim SB, Jeong YD. An analysis of grinding power and surface roughness in external cylindrical grinding of hardened SCM440 steel using the response surface method. *Int J Mach Tools Manuf* 2006;46:304–12.
- [24] Al-Ahmari AMA. Predictive machinability models for a selected hard material in turning operations. *J Mater Process Technol* 2007;190:305–11.
- [25] HÖktem H, Erzurumlu T, Kurtaran H. Application of response surface methodology in the optimization of cutting conditions for surface roughness. *J Mater Process Technol* 2005;170:11–6.
- [26] Benga GC, Abrão AM. Turning of hardened 100Cr6 bearing steel with ceramic and PCBN cutting tools. *J Mater Process Technol* 2003;143:237–41.
- [27] Suresh PVS, Venkateswara RP, Deshmukh SG. A genetic algorithmic approach for optimization of surface roughness prediction model. *Int J Mach Tools Manuf* 2002;42:675–80.
- [28] Kwak JS. Application of Taguchi and response surface methodologies for geometric error in surface grinding process. *Int J Mach Tools Manuf* 2005;45:327–34.
- [29] Montgomery DC. Design and analysis of experiments. 4th ed. New York: Wiley; 2001.
- [30] Derringer G, Suich R. Simultaneous optimization of several response variables. *J Qual Technol* 1980;12:214–9.
- [31] Ardakani MK, Noorossana R. A new optimization criterion for robust parameter design — the case of target is best. *Int J Adv Manuf Technol* 2008;38:851–9.
- [32] Kulkarni MS, Mariappan V. Multiple response optimization for improved machined surface quality. *J Mater Process Technol* 2003;141:174–80.
- [33] Lin DKJ, Tu W. Dual response surface optimization. *J Qual Technol* 1995;27:34–9.
- [34] Köksoy O. Multiresponse robust design: mean square error (MSE) criterion. *Appl Math Comput* 2006;175(2):1716–29.
- [35] Vining GG, Myers RH. Combining Taguchi and response surface philosophies: a dual response approach. *J Qual Technol* 1990;22:38–45.
- [36] Köksoy O, Yalcinoz T. Mean square error criteria to multiresponse process optimization by a new genetic algorithm. *Appl Math Comput* 2006;175(2):1657–74.
- [37] Chiao H, Hamada M. Analyzing experiments with correlated multiple responses. *J Qual Technol* 2001;33:451–65.
- [38] Wu FC. Optimization of correlated multiple quality characteristics using desirability function. *Qual Eng* 2005;17(1):119–26.
- [39] Box GEP, Hunter WG, MacGregor JF, Erjavec J. Some problems associated with the analysis of multiresponse data. *Technometrics* 1973;15(1):33–51.
- [40] Khuri AI, Conlon M. Simultaneous optimization of multiple responses represented by polynomial regression functions. *Technometrics* 1981;23(4):363–75.
- [41] Bratchell N. Multivariate response surface modeling by principal components analysis. *J Chem* 1989;3:579–88.
- [42] Paiva AP, Costa SC, Paiva EJ, Ferreira JR, Balestrassi PP. Multi-objective optimization of pulsed gas metal arc welding process based on weighted principal component scores. *Int J Adv Manuf Technol* 2010;50:113–25.
- [43] Tzeng YF, Chen FC. Multiobjective process optimization for turning of tool steels. *Int J Mach Mach Mater* 2006;1:76–93.
- [44] Tzeng YF. A hybrid approach to optimize multiple performance characteristics of high-speed computerized numerical control milling tool steels. *Mater Des* 2007;28(1):36–46.
- [45] Fung CP, Kang PC. Multi-response optimization in friction properties of PBT composites using Taguchi method and principal component analysis. *J Mater Process Technol* 2005;170:602–10.
- [46] Liao HC. Multi-response optimization using weighted principal components. *Int J Adv Manuf Technol* 2005;27:720–5.
- [47] Johnson RA, Wichern D. Applied multivariate statistical analysis. 5th ed. New Jersey: Prentice-Hall; 2002.



Paulo Henrique da Silva Campos is an Industrial Engineering PhD student of Federal University at Itajuba/Brazil. His interest lies on Design an Analysis of Experiments and Manufacturing Process Optimization.



João R. Ferreira is Associate Professor of manufacturing processes in the Institute of Industrial Engineering of the Federal University of Itajuba, Brazil. He received the doctor degree in mechanical engineering in 1999 at the State University of Campinas, Brazil. His research interests are in machining process optimization and statistics.



Luiz Gustavo Dias Lopes is professor of the Industrial Engineering Department of the Universidade do Vale do Sapucaí — UNIVAS/Brazil. He is also a PhD student of Industrial Engineering at the Federal University of Itajuba/Brazil. His area of interest is Design and Analysis of Experiments and multivariate optimization.



Emerson José de Paiva is professor of Simulation and Optimization on the Federal University of Itajuba/Brazil. He is also a PhD student of Industrial Engineering at the Federal University of Itajuba/Brazil. His area of interest is Design and Analysis of Experiments and multivariate optimization.



Pedro P. Balestrassi received the D.Sc. degree in Industrial Engineering from the Federal University of Santa Catarina, Brazil, in 2000. Since 1994, he has been with the Federal University of Itajuba, Brazil, as Professor of Industrial Engineering. In 1998/1999, he was visitor at Texas A&M University (TX, USA) and in 2005/2006 he was visiting the University of Texas at Austin. He is now visiting scholar at the University of Tennessee. His areas of interest lie in times series forecasting, ANN and statistics.



Anderson Paulo de Paiva is Professor of Quantitative Methods in the Industrial Engineering Institute of the Federal University at Itajuba, Brazil. He received the D.Sc. degree in Mechanical Engineering in 2006 at the Federal University of Itajuba, Brazil. His research interests are in Multivariate Statistical Analysis, Nonlinear Optimization and Neural Networks applied to manufacturing processes.